Transcorneal Electrical Stimulation Reduces Neurodegenerative Process in a Mouse Model of Glaucoma

ASSRAA HASSAN JASSIM,[1,5] MCKAY CAVANAUGH,[2] JESSICA STUKEL SHAH,[2]
REBECCA WILLITS [2,3] and DENISE M. INMAN[1,4]

[1]Department of Pharmaceutical Sciences, Northeast Ohio Medical University, Rootstown, OH, USA; [2]Department of Biomedical Engineering, University of Akron, Akron, OH, USA; [3]Department of Chemical Engineering, Northeastern University, Boston, MA, USA; [4]North Texas Eye Research Institute, UNT-HSC, 3500 Camp Bowie Blvd, Fort Worth, TX 76107, USA; and [5]Department of Basic and Translational Sciences, University of Pennsylvania, Philadelphia, PA, USA

Abstract—Glaucoma is a neurodegenerative disease in which the retinal ganglion cell axons of the optic nerve degenerate concomitant with synaptic changes in the retina, leading finally to death of the retinal ganglion cells (RGCs). Electrical stimulation has been used to improve neural regeneration in a variety of systems, including in diseases of the retina. Therefore, the focus of this study was to investigate whether transcorneal electrical stimulation (TES) in the DBA2/J mouse model of glaucoma could improve retinal or optic nerve pathology and serve as a minimally invasive treatment option. Mice (10 months-old) received 21 sessions of TES over 8 weeks, after which we evaluated RGC number, axon number, and anterograde axonal transport using histology and immunohistochemistry. To gain insight into the mechanism of proposed protection, we also evaluated inflammation by quantifying $CD3^+$ T-cells and $Iba1^+$ microglia; perturbations in metabolism were shown *via* the ratio pAMPK to AMPK, and changes in trophic support were tested using protein capillary electrophoresis. We found that TES resulted in RGC axon protection, a reduction in inflammatory cells and their activation, improved energy homeostasis, and a reduction of the cell death-associated p75NTR. Collectively, the data indicated that TES maintained axons, decreased inflammation, and increased trophic factor support, in the form of receptor presence and energy homeostasis, suggesting that electrical stimulation impacts several facets of the neurodegenerative process in glaucoma.

Address correspondence to Denise M. Inman, North Texas Eye Research Institute, UNT-HSC, 3500 Camp Bowie Blvd, Fort Worth, TX 76107, USA. Electronic mail: Denise.inman@unthsc.edu; Rebecca Willits, Department of Chemical Engineering, Northeastern University, Boston, MA, USA. Electronic mail: r.willits@northeastern.edu

Assraa Hassan Jassim and McKay Cavanaugh have contributed equally to this work.

INTRODUCTION

Glaucoma is an optic neuropathy that encompasses a group of neurodegenerative diseases, ultimately resulting in irreversible blindness due to retinal ganglion cell (RGC) dysfunction and degeneration. The pathophysiology of glaucoma, especially the window of time between initial changes in the retinogeniculate pathway and overt retinal ganglion cell loss, offers an opportunity for therapeutic intervention. Currently, there is no cure for glaucoma and all therapies target lowering the intraocular pressure (IOP), an important risk factor yet not causative for the disease.[41] Given that patients with glaucoma may have to manage their disease for up to 50 years, direct benefit would come from therapies that are longitudinal and non-invasive. In glaucoma, the breakdown of visual function occurs at the bipolar to RGC synapse[37]; the RGC to magno- and parvo-cellular cell synapses in the lateral geniculate nucleus (LGN)[20]; and synaptic changes in the superior colliculus, the major retino-recipient region for rodents. In addition to synaptic loss, RGC axons degenerate within the optic nerve.[39] Treatment strategies, including electrical stimulation, may contribute to slowing disease progression.

Current glaucoma therapies target reduction in IOP; however, none have been proven to restore vision. The use of electrical stimulation has been shown to have a

© 2020 Biomedical Engineering Society

neuroprotective effect in multiple tissue types and has been used as a minimally invasive treatment option for several diseases. These treatments have been explored to yield functional improvement in humans. Patients with non-arteritic ischemic optic neuropathy showed preserved visual acuity thresholds 3 months after a single transcorneal electrical stimulation (TES) treatment.[15] Similarly, 30 min of TES improved visual acuity in some eyes and increased focal electroretinogram output 1 month after treatment in patients with branch retinal artery occlusion.[36] In a clinical trial, transorbital stimulation was used for 50 min a day for 10 days in patients with optic neuropathies, including glaucoma. After stimulation, a transient increase in visual fields and decrease in reaction time was found, however there was no improvement in visual acuity.[16] While not all patients benefit from electrical stimulation treatment, incrementally better vision after stimulation should not be dismissed—non-invasive techniques that can improve vision for patients by any degree can have a major impact on quality of life. To increase the efficacy of TES, a greater understanding of the mechanism of neuroprotection must be established.

Similar to human studies, TES in rodent models has shown efficacy for various diseases of the eye, yet the mechanism of action remains unclear. Several studies point to changes in pathology that could influence glaucoma trajectories. For example, morphological changes, such as photoreceptor survival and preservation of retinal function, were seen in rats with retinitis pigmentosa after TES.[32] Increased trophic support or reduction in microglial activation was also found following TES in rats.[33,35,47] These studies demonstrated a positive effect on visual function following TES and hint at potential mechanisms of action. However, efficacy following TES in models of glaucoma is needed to further explore potential mechanisms of any improvement.

Therefore, the purpose of this study was to assess the use of TES to treat glaucoma pathology in a rodent model. In this study, we examined the effectiveness of TES in treating retinal and axonal degeneration that underlies vision loss during glaucoma. The DBA2/J mouse model was subjected to 8 weeks of TES. The effect of stimulation on the visual system was evaluated by examining RGC survival, the integrity of the optic nerve and perturbations in inflammation, metabolism, and trophic support that occurred throughout the system. Our results indicated that TES is a minimally invasive treatment option to target aspects of glaucoma pathology.

METHODS

Materials

Beuthanasia-D (07-807-3963, Merck Animal Health, Madison, NJ), phosphate buffered saline (PBS) (BP3994, Fisher Scientific, Waltham, MA), paraformaldehyde (PFA) (BP531 Fisher Scientific, Waltham, MA), methylcellulose eye drop solution (Alcon, Geneva, Switzerland), Fluoromount-G (0100, Southern Biotech, Birmingham, AL). FluoroGold (hydroxystilbamidine; FG; 22845, by Invitrogen through ThermoFisher Scientific, Waltham, MA), Araldite 502/Polybed 812 kit (08791; Polysciences, Inc, Warrington, PA, USA), T-PER buffer (78510, ThermoFisher Scientific, Waltham, MA), HALT protease and phosphatase inhibitor cocktail (78442, by Pierce, through ThermoFisher Scientific, Waltham, MA), Bicinchoninic Acid Protein Assay Kit (BCA, by Pierce through ThermoFisher Scientific, Waltham, MA), cholera toxin B subunit (CTB conjugated to AlexaFluor-488; C22841, Invitrogen, Carlsbad, CA), donkey serum (DKS) 017-000-121, Jackson ImmunoResearch, West Grove, PA, USA).

Antibodies: C-fos (sc-166940, Santa Cruz Biotechnology, Dallas, TX); RBPMS (GTX118619, Genetex, Irvine, CA); Iba1 (NC9288364, by Wako through Fisher Scientific, Waltham, MA); CD3 (MAB4841, R&D Systems, Minneapolis, MN); β-actin (ab8227 Abcam, Boston, MA); p75 (sc-271708, SantaCruz Biotechnology, Dallas, TX); TrkB (sc-377218, Santa Cruz Biotechnology, Dallas, TX); pTrkB (ABN1381, Millipore-Sigma, St. Louis, MO); brain-derived neurotrophic factor (BDNF, sc-65514, Santa Cruz Biotechnology, Dallas, TX); AMP kinase and phosphorylated AMP kinase (AMPK, NBP2-22127, and pAMPK NBP1-74502, Novus Biologicals, Littleton, CO). Secondary antibodies were appropriate AlexaFluor conjugates from Jackson ImmunoResearch, West Grove, PA. DAPI (D1306, ThermoFisher Scientific, Waltham, MA).

Animals

All procedures were approved by the Institutional Animal Care and Use Committee and performed in accordance with the ARVO Statement for the Use of Animals in Ophthalmic and Vision Research. The glaucoma model for the study was the DBA/2 J (D2) mouse strain. The D2 mouse develops an iris pigment dispersion disease that leads to increased IOP and eventual loss of RGCs.[27] All mice were originally

obtained from Jackson Laboratories (Bar Harbor, ME, USA) and housed in an animal care facility with a 12-hour light/dark schedule, ambient air temperature of 69–79 °F and 30–70% humidity. All mice had free access to standard laboratory rodent food and water. Both males and females were used. Mice were divided into three groups: (1) Control Non-stimulated D2, ($n = 25$); (2) Stimulated D2, ($n = 18$); and (3) Control D2, ($n = 8$). One control group was matched for age (Control Non-stimulated) and the other for strain; Control D2 were 3 to 5 months (m) of age. These ages were chosen because the onset of glaucoma-associated pathology occurs between the ages of 8–9 months in the D2 mouse; therefore, the use of a 10-month-old animal represented the disease phenotype. The 3 to 5-month-old D2 control group represented the pre-disease phenotype.

Figure 1 shows the overall experimental design. Animals were divided into 2 groups (experimental and control) with statistically equivalent IOP measurements. The experiment was conducted over the course of 8 weeks, after which animals were further randomly divided into various endpoint evaluations. A separate subset of mice ($n = 4$) were examined for c-fos, an intermediate early gene upregulated in response to stimulation, to confirm activation in the brain due to TES.[43] Some mice (23 mice with each eye measured, $n = 46$) were examined for retrograde labeling from the superior colliculus to the eye and another subset of mice (16 mice with each eye measured, $n = 32$) were examined for anterograde transport from the eye to the superior colliculus. All mice ($n = 51$) were sacrificed approximately 3 days after the final stimulation with an overdose of Beuthanasia-D and transcardially perfused with 0.1 M PBS followed by 4% PFA except as noted below. Brain, optic nerve, and eyes were collected for cellular and protein analysis.

IOP Measurements

IOP measurements, measured in mmHg, were taken for both eyes in all mice before stimulation (0 weeks) as a baseline, to assure statistical equivalence for group distribution, and after stimulation at the final time point (8 weeks). Mice were lightly anesthetized using 2.5% isoflurane and a total of 10 measurements per eye were taken using a TonoLab rebound tonometer (iCare Finland Oy, Vantaa, Finland). The 10 IOP measures were taken at approximately the same time each measurement day then averaged together for each eye.

Stimulation Paradigm

TES was applied to both mouse eyes in the Stimulated 12 m D2 group for 10 min every 3 days for 8 weeks. Contact lens electrodes were made according to the
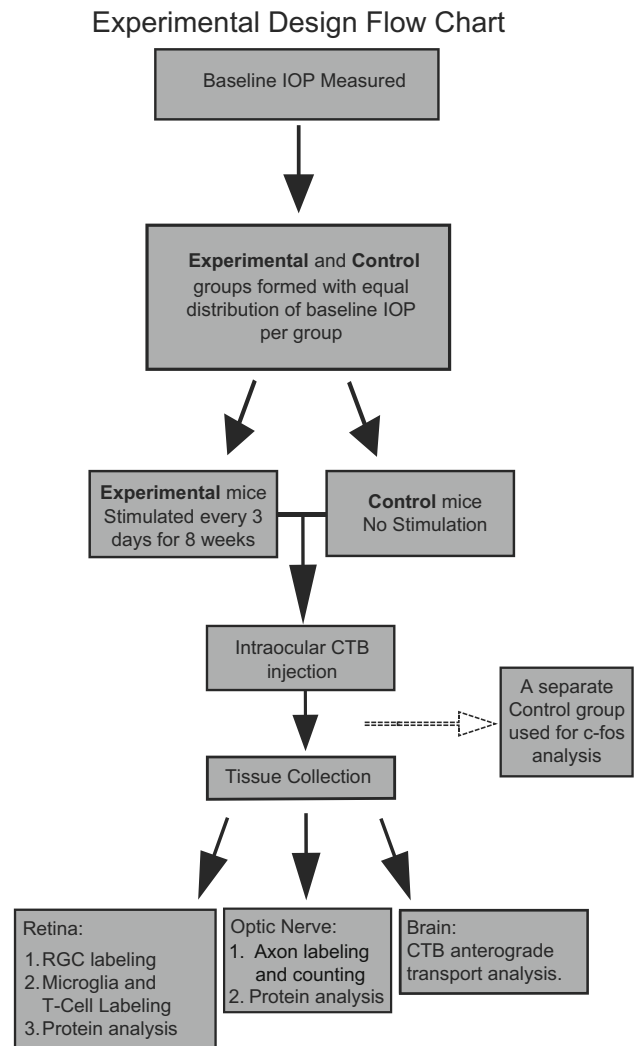
Experimental Design Flow Chart

FIGURE 1. Experimental design. Baseline IOP was established in mice and used to divide animals into experimental and control groups. Stimulation was administered to experimental mice every 3 days for 8 weeks; control mice received no treatment. At the end of 8 weeks, final IOP measures were taken and CTB was intravitreally injected 2–3 days prior to sacrifice. After sacrifice, retina, optic nerve (ON) and superior colliculus (SC) were collected for analysis of retinal ganglion cell soma and axon survival. A separate group of mice were used for c-fos analysis.

protocol described[40]; briefly, lenses were cut from ACLAR embedding film (Electron Microscopy Sciences, Hatfield, PA) to be approximately 3 mm in diameter. A 10 cm piece of silver-coated 22/1-denier nylon fiber (Statex Produktions-und Vertriebs GmbH, Bremen, Germany) was threaded on the inner side of the contact lens. Animals were then anesthetized using 2.5–3% isoflurane and placed on a heating pad for the duration of stimulation. The contact was placed on the eye of the animal with approximately 10 μl of methylcellulose eye drop solution to ensure constant contact with the eye.

Each eye was stimulated separately with a ground wire placed in the back of the neck. A Master 8 power supply (World Precision Instruments) and isolator (World Precision Instruments) were used to apply TES, consisting of a symmetric biphasic square wave at a current of 100 μA, 1 ms pulse duration, at a frequency of 20 Hz, for 10 min. After 10 min, the electrode was moved the other eye and TES was applied. Contacts were cleaned with ethanol and DI water following stimulation of each mouse. During this time, Control 12 m D2 and Control 5 m D2 mice received no stimulation.

Analysis of c-fos Activation

Labeling for the immediate early gene c-fos occurs in the nucleus and is optimally observed 90 min post-stimulation of the retina. A separate group of experimental D2 mice ($n = 4$) were used to evaluate the activation of c-fos. A positive control ($n = 1$) was generated by creating osmotic thirst *via* an intraperitoneal injection of 4% saline solution. A negative control ($n = 1$) was a D2 mouse without stimulation. Mice were anesthetized with 2.5% isoflurane and stimulation was applied as described in the above protocol. Mice were sacrificed 90 min post stimulation and transcardially perfused with 0.1 M PBS then 4% PFA. Brains were collected and post-fixed overnight in 4% PFA. Brains were sectioned at 50 μm on a Leica freezing microtome (Wetzlar, Germany) and stored in PBS-sodium/azide for immunohistochemical analysis. The tissue was washed then blocked in 5% donkey serum (DKS) and 1% Triton X-100 in PBS-sodium azide followed by 48 h of incubation at 4 °C in c-fos primary antibody diluted (1:800) in 3% DKS and 1% Triton X-100 in PBS-sodium azide. After washing in PBS-azide, sections were incubated in secondary antibody conjugated to Alexa Fluor 594 diluted (1:300) in 1% DKS and 1% Triton X-100 in PBS-sodium azide overnight at room temperature. After a final wash, six representative sections were mounted on SuperFrost slides and coverslipped with Fluoromount-G. Sections were imaged with a Leica confocal DMi8 microscope (Leica Microsystems, Buffalo Grove, IL, USA). The negative control was imaged to establish background fluorescent intensity settings, then the positive control and c-fos stained samples were imaged to view c-fos activation based on the negative control settings. The positive control was used as a reference for c-fos activation. Images for presentation were taken on an Observer Z1 inverted microscope (Zeiss Microscopy, White Plains, NY).

Retrograde RGC Labeling and Quantification

FluoroGold (FG) was used to retrogradely label RGCs in a subset of control and experimental study mice. Five days prior to sacrifice, mice ($n = 23$) were anesthetized using 3% isoflurane and placed in a stereotaxic apparatus. Using coordinates ($- 4.4$ mm posterior to Bregma, ± 0.5 mm lateral, and 0.5 mm below skull surface), 1.5 μl of 3% FG in 10% dimethyl sulfoxide/PBS was injected bilaterally into each superior colliculus (SC). Five days after intracranial injections, mice were euthanized as described above. Eyes were dissected out and allowed to postfix in PFA for 1 h before being stored in 30% sucrose in 0.1 M PBS. Retinas were dissected out, relief cuts made, then mounted onto glass slides, and coverslipped. Whole mount images were obtained by stitching together z-stacked tiles of the retina at 160$\times$ magnification on a Zeiss AxioZoom fluorescent microscope. FG labelled RGCs were quantified using ImagePro (Media Cybernetics, Inc; Rockville, MD) after processing the images through 2-D filters to sort fluorescently labelled cells of a certain size and shape and also eliminate any artifacts.[13] ImagePro was also used to calculate retinal areas. The total number of cells was then divided by the area of the retina to give a measure of RGC density.

Analysis of Anterograde Transport

Three days prior to sacrifice, mice from the experimental and control groups were anesthetized using 2.5% isoflurane and received an intraocular injection of 1.5μL CTB conjugated to Alexa Fluor-488. CTB is taken up by the RGCs and transported *via* endocytic vesicles to the superior colliculus (SC).[13] SC was harvested for analysis after mice were sacrificed and perfused. Retinas were dissected out and mounted onto glass slides then coverslipped. The whole mount retinas were checked to ensure proper administration of the CTB injection and uptake by the RGCs. The SC was coronally sectioned at 50 μm on a Leica freezing microtome (Wetzlar, Germany). Representative sections (choosing every third section from the sectioned tissue, up to 10 total) were mounted and imaged at 40$\times$ using a Zeiss Axiozoom V16 (AxioCam MRm Rev.3; Zeiss, Jena, Germany). Each side (right and left) of the SC was imaged and analyzed separately. ImageJ[42] was then used to analyze the percent area fraction (PAF) of CTB labeling in each SC section *via* a custom macro script[13] that measured the relative intensity of binned pixels in a defined area of interest with the background fluorescence subtracted. The intensity values were summed then normalized by the

number of bins to obtain the PAF for the right and left SC of each animal.

Optic Nerve Histology

Distal portions of optic nerves (ONs), 50% of the myelinated optic nerve that is roughly 2500 μm beyond the globe, were post fixed in 2% PFA and 2% glutaraldehyde in 0.1 M sodium cacodylate buffer (CB; pH 7.4) for 48 h. Tissue was processed as previously described.[11] Following fixation, ONs were stored in 0.1 M cacodylate buffer until incubation in 2% osmium tetroxide on ice for 45 min, after which nerves went through a series of dehydration steps in ethanol and propylene oxide. Incubations in increasing concentrations of PolyBed resin mixed with propylene oxide culminated in final embedding and polymerization in PolyBed resin under vacuum before final placement in molds for hardening in a 60 °C oven. Next, 500 nm sections for each nerve were cut on an ultramicrotome (Leica). Sections were mounted on slides and stained with 1% ρ-phenylenediamine to visualize the axons and any degenerative debris. Imaging and quantification of the samples are detailed in the Cell and Axon Quantification section below.

Immunohistochemistry

For sectioned tissue Globes were cryoprotected in 30% sucrose in 0.1 M PBS sodium azide, at minimum overnight, then embedded in OCT and sectioned at 10 μm on a Leica cryostat. Sections were collected onto SuperFrost slides (Fisher Scientific, Waltham, MA). *For wholemounts* Retina, dissected from PBS-perfused animals, were fixed in 4% PFA for 15–30 min then kept in 0.1 M PBS sodium azide until vitreous removal.

Both sectioned tissue and wholemounts were washed in 0.1 M PBS then blocked for 1 h at room temperature with 5% DKS and 0.4% Triton X-100 in 0.1 M PBS. The tissue was then incubated in the primary antibody overnight (sectioned tissue) or 48 h (wholemounts) at 4 °C; primary antibodies were diluted in blocking solution. Tissue was washed in 0.1 M PBS, blocked for 30 min, then incubated in secondary antibody diluted 1:250 in blocking solution for 2 h at room temperature. After an additional 0.1 M PBS rinse, tissue was labeled with DAPI (1:2000) in tris buffered saline for 10 min. Slides were rinsed then coverslipped with Fluoromount-G.

Cell and Axon Quantification

RBPMS-labeled RGCs and ρ-phenylenediamine stained RGC axons were quantified using unbiased stereological analysis.[29] In both cases, cell or axon quantification was performed as previously described using the optical fractionator module within StereoInvestigator (MicroBrightfield Bioscience, Williston, VT).[23,26] A 50 x 50 μm or 5 x 5 μm counting frame (retina or ON, respectively) was used across approximately 40 sites (10%) for both tissue types. The coefficient of error (Schmitz-Hof) was maintained at 0.05 or below, ensuring sufficient sampling rate.

Inflammation in Retina

Microglia immunolabeled with Iba1 were quantified by counting the cell bodies of Iba1$^+$ cells that were colocalized with DAPI in the ganglion cell and inner plexiform layers (GCL and IPL) from 6 sagittal retinal sections per animal. A minimum of 35 random regions (5 μm $\times$ 5 μm) of interest were evaluated over the inner retina for the section. The number of Iba1 positive microglia within the sampling area per retinal section was averaged per animal and expressed as Iba1$^+$ cells per μm. CD3$^+$ T cells were also quantified in the IPL and GCL of retina from 3 sagittal sections per retina, then averaged for each animal. T cells are expressed as CD3$^+$ cells per retina.

Iba1 immunolabel intensity is proportional to the activation state, so measuring the labeling intensity can be a proxy for microglial activation. All images were taken using the same timing and level of exposure, then analyzed using ImageJ. The ImageJ PAF macro (see above) was applied to quantify Iba1 label intensity in the IPL of retina. One image per section was taken of 6 sagittal sections per mouse. The obtained PAFs from all sections were averaged for each animal.

Protein Quantification

Retinal and myelinated ON proteins were collected into tubes containing Tissue Protein Extraction Reagent buffer with HALT protease and phosphatase inhibitors, then disrupted with a Branson Sonifier (3-second pulse at 10% amplitude) to create a protein lysate. Total protein concentration was measured by BCA assay kit.[26] AMP kinase and phosphorylated AMP kinase were analyzed by capillary tube–based electrophoresis immunoassay using the Wes, a Protein Simple instrument that separates proteins by electrical charge in capillary tubes and allows binding of primary antibody then protein visualization within the capillary.[26] All other proteins were analyzed by western blot. Proteins separated by electrophoresis on denaturing polyacrylamide gels were transferred to a polyvinyl difluoride membrane. Blots were probed with antibodies against β-actin, p75, TrkB, pTrkB, and BDNF (1:1000). Appropriate secondary antibodies
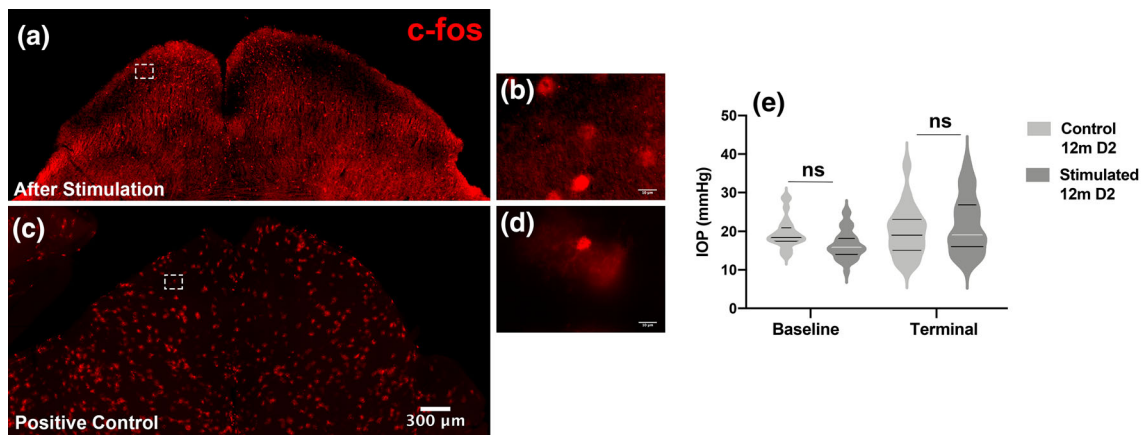
FIGURE 2. Effect of Stimulation Paradigm. (a) C-fos, an immediate early gene immunolabeled (red) in a section of midbrain from a mouse stimulated using our TES paradigm (scale bar is 300 μm). (b) White box outlines a portion of the superior colliculus that is shown at higher magnification in the inset (scale bar is 30 μm). (c) Midbrain section from a mouse subjected to a hyperosmotic solution (IP) for the c-fos positive control (no stimulation; scale bar is 300 μm). (d) Inset shows c-fos activation at higher magnification (scale bar is 30 μm). (e) IOP (mmHg) was measured prior to stimulation (baseline) and after 8-weeks (final). Ten IOP measurements were taken per eye and averaged; no significant differences were found between the groups. Control 12 m D2, $n = 22$; Stimulated 12 m D2, $n = 35$.

conjugated to horseradish peroxidase were used, then visualized with chemiluminescence (Pierce, Rockford, IL, USA). Band density was measured using the lane profile analysis function in AlphaView SA version 3.4.0 software and normalized to β-actin within lane band density.[26]

Statistical Analysis

All results are represented as violin plots to show distribution of data and evaluated for normalcy; $p < 0.05$ was considered statistically significant. Statistical evaluation was completed using GraphPad Prism 8 (GraphPad, San Diego, CA, USA). Student's t test was used when comparing two groups; three or more group comparisons used a one-way ANOVA followed by a general linear model (GLM). Tukey's honestly significant difference post hoc test was used to perform multiple comparisons among groups. A non-parametric Mann–Whitney test was used to compare two groups that were not normally distributed. For comparisons of three groups that did not meet the assumption for ANOVA, a Kruskal–Wallis Test was performed with a Dunn's multiple comparisons post hoc test. Images used for results presentation are from representative samples, determined by choosing images from the third quartile of each respective analysis.

RESULTS

Figure 1 shows the experimental design. Mice in the Stimulated group received TES for 10 min per eye every 3 days over 8 weeks. To determine the effec-

tiveness of the stimulation paradigm, we first examined the activation of c-fos in the SC. Immunolabeling for c-fos was evident in the SC after 10 min of 20 Hz stimulation of mouse eyes through a wired contact lens (Figs. 2a and 2b), indicating that the stimulation activated RGCs to a degree that led to downstream activation of cells in the superficial layers of the SC; Figs. 2c and 2d show the positive control.

Baseline IOP measures were used to randomize mice into their respective Control and Stimulated groups. At the end of the 8 weeks of stimulation, terminal IOP measurements were collected (Fig. 2e). Both Control and Stimulated 12 m D2 mice had IOP that did not differ, indicating the stimulation did not impact IOP. Although IOP elevation is one of the main risk factors of glaucoma, IOP lowering drugs can slow, but not prevent RGC degeneration. This indicates that the mechanism of degeneration goes beyond IOP elevation, so efforts to protect RGCs that do not affect IOP, as demonstrated here for TES, will be important additions to therapeutic options.

Effect of TES on RGC Survival

To observe the effect of TES on the retina and ON, we quantified RGCs, their axons, and measured anterograde axonal transport. Both the Control 12 m D2 and Stimulated 12 m D2 had significantly decreased RGC density compared to the healthy Control 5 m D2 (Figs. 3a and 2b–d).

While no difference was found with RGC number, TES had a positive effect on axon survival. Stimulated 12 m D2 ON had significantly more axons compared to the Control 12 m D2 group (Fig. 3e) quantified
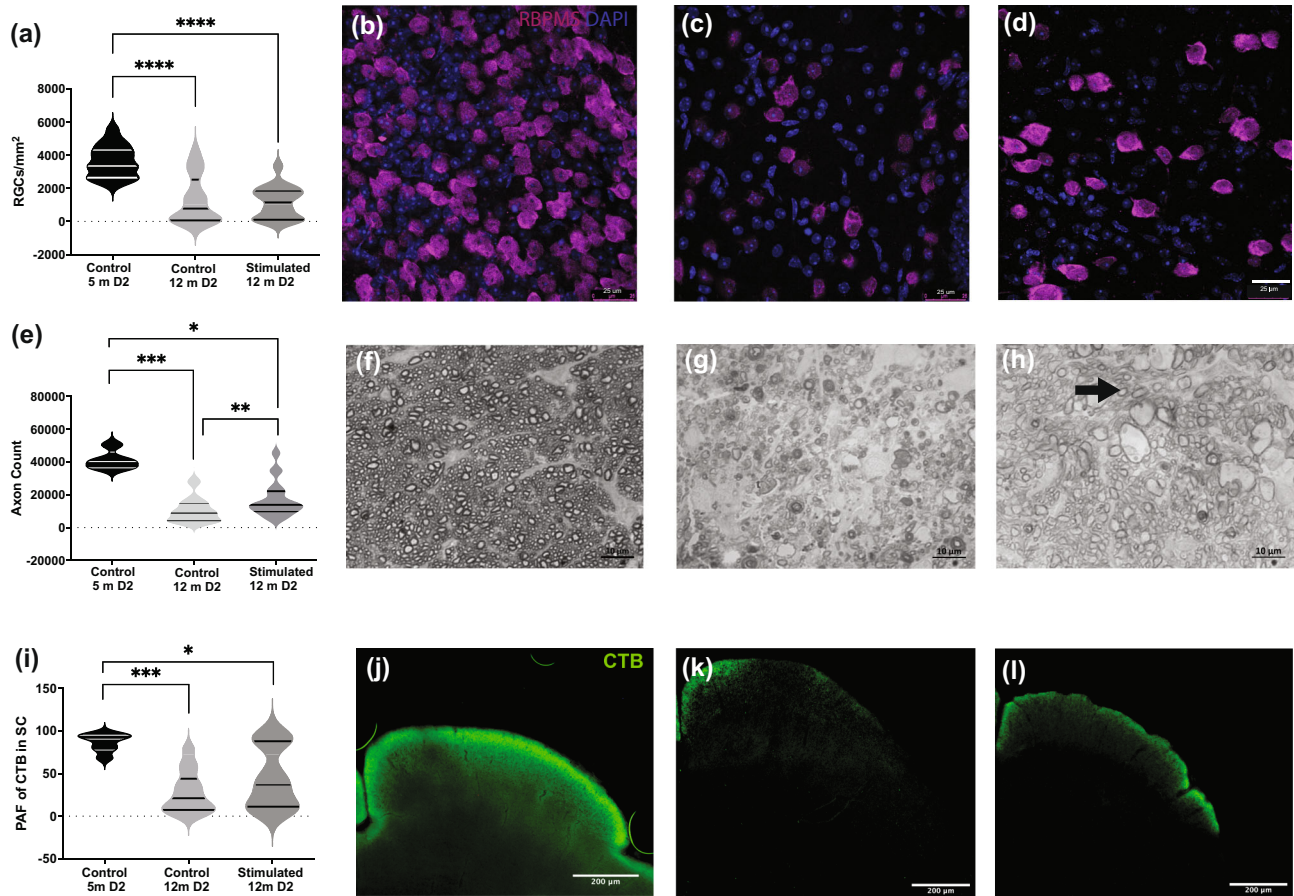
FIGURE 3. TES slows glaucoma pathology (a). RBPMS and FG-positive RGC somata in whole mount retina were quantified using unbiased stereology. There were significantly more RGCs in the Control 5 m D2 ($n = 19$) compared to the Control 12 m D2 ($n = 22$) and the Stimulated 12 m D2 ($n = 18$) ($p < 0.0001$ and $p < 0.0001$ respectively). (b–d) Immunohistochemistry of RGCs (RBPMS, magenta; DAPI, blue) in whole mount retina, with representative images from each group (b Control 5 m D2; c Control 12 m D2; d Stimulated 12 m D2). Scale bars = 25 μm. E. Unbiased stereological axon count of stained cross-sections of ON from Control 5 m D2 ($n = 5$), Control 12 m D2 ($n = 40$) and Stimulated 12 m D2 ($n = 32$) show Control 5 m D2 ON had significantly more axons than both Control 12 m D2 and Stimulated 12 m D2 ($p = 0.0001$ and $p = 0.0288$ respectively). Stimulated 12 m D2 samples also showed significantly more axons compared to Control 12 m D2 samples ($p = 0.0074$). (f–h) Representative images of stained cross-sections of ON for each group (F. Control 5 m D2; G. Control 12 m D2; H. Stimulated 12 m D2) show degenerating axons (red arrow) in Control 12 m D2. Black arrows in panels for Stimulated 12 m D2 and Control 5 m D2 point to healthy axons. Scale bars = 10 μm. I. CTB transport to the SC was significantly higher in the Control 5 m D2 ($n = 7$) compared to the Control 12 m D2 ($n = 27$) and Stimulated 12 m D2 ($n = 16$) ($p = 0.0005$ and $p = 0.0301$ respectively). (j–l) Representative images of CTB labeling (green) in coronal sections of SC show axonal transport from retina to SC of Control 12 m D2 and Stimulated 12 m D2 mice (J. Control 5 m D2; K. Control 12 m D2; L. Stimulated 12 m D2). Scale bars = 200 μm.

from images (Figs. 3f–3h) with healthy axons denoted by black arrows in the Control 5 m D2 and the Stimulated 12 m D2. Axons in the Control 12 m D2 group (red arrow) showed significant degeneration and gliosis, which is shown the increased size of the astrocyte somas and the larger processes between fascicles as previously detailed in D2 glaucomatous ON.[7,10]

Injection of CTB into the eye prior to mouse sacrifice was used to examine anterograde axonal transport. The percent area fraction (PAF) of the SC labeled by CTB showed significant loss of axonal transport in both the Control and Stimulated 12 m D2

compared to the Control 5 m D2 (Fig. 3l). No statistical difference in transport between Control and Stimulated 12 m D2 was observed. Representative images of the SC from both Control and Stimulated 12 m D2 groups, with CTB in green, are shown (Figs. 3j–3l). Whole mount retinas from the corresponding eyes for either the Control or Stimulated 12 m D2 groups were viewed to confirm complete CTB distribution across the ganglion cell layer of the retina. Thus, disruption of CTB transport from the retina to the SC can be attributed to failures in transport, not technique.
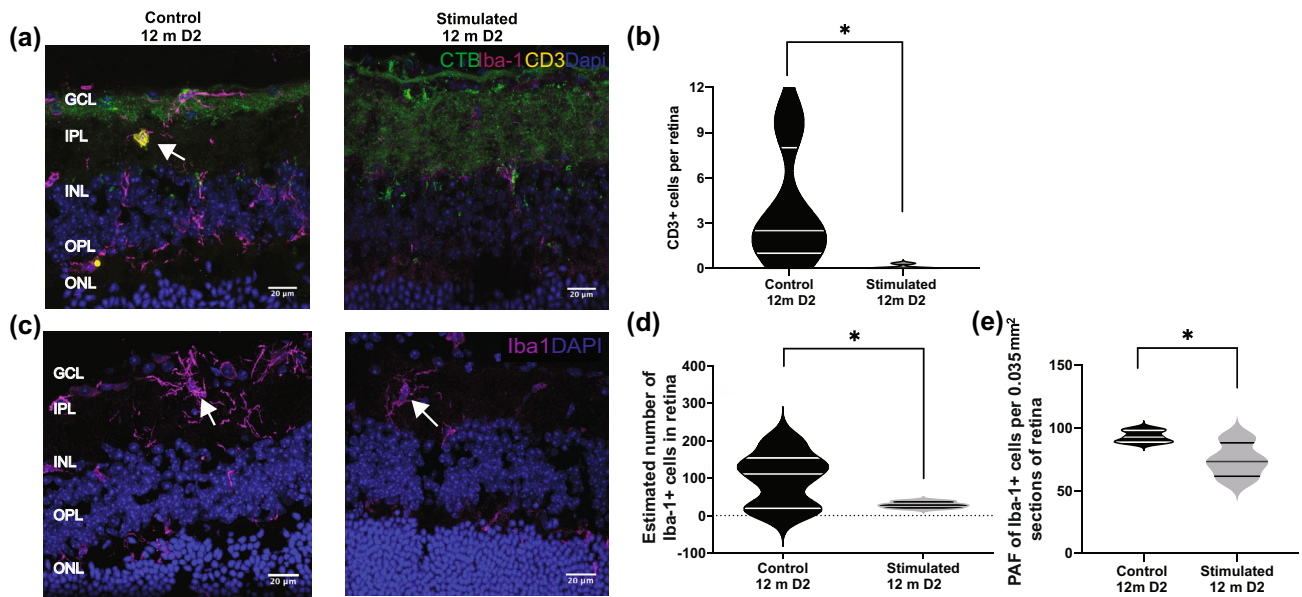
FIGURE 4. TES reduces inflammation (a). Sagittal sections of retina show CD3$^+$ T cells (yellow; white arrow) in representative images of Control 12 m D2 and no T cells in the Stimulated 12 m D2 retina. CTB (green), Iba-1 (magenta), and DAPI (blue). (b) Quantification of CD3$^+$ T cells found in the retina of Stimulated 12 m D2 ($n = 4$) compared to the Control 12 m D2 ($n = 4$) showing a reduction in CD3$^+$ T cells in the stimulated group ($p = 0.0286$). (c) Microglia expressing Iba1 (magenta and white arrow) in the IPL and GCL of retina in Control 12 m D2 and Stimulated 12 m D2 samples. DAPI (blue). GCL = ganglion cell layer, IPL = inner plexiform layer, INL = inner nuclear layer, OPL = outer plexiform layer (OPL), and ONL = outer nuclear layer. (d) Decreased inflammation shown by a significant reduction in the number of Iba1$^+$ microglia in the IPL and GCL of Stimulated 12 m D2 mice ($p = 0.0467$). (e) Reduced inflammation also shown by a significant reduction in the percent area fraction (PAF) of Iba1$^+$ immunolabeling in the Stimulated 12 m D2 compared to the Control 12 m D2 retina ($n = 4$ and $n = 6$ respectively; $p = 0.0135$).

Decreased Inflammation in TES Retina

Inflammation plays a major role in glaucoma progression. Thus, to determine whether TES impacted the inflammatory response, we evaluated whether T cells had infiltrated the retina using immunolabeling for CD3 (yellow, and with white arrow, Fig. 4a). CD3$^+$ T cells were quantified in sectioned retina for the Control and Stimulated 12 m D2 groups (Fig. 4b). CD3$^+$ T cells were found in significantly higher numbers in the Control 12 m D2 group.

Figure 4c shows representative sections of Iba1 immunolabeling in Control and Stimulated 12 m D2 retina. We also quantified Iba1$^+$ microglia (Fig. 4d), finding a significant decrease in number for the Stimulated compared to the Control 12 m D2 group. The percent area fraction (PAF) of inner retina that was labeled with Iba1$^+$ microglia was significantly higher for Control 12 m D2 mice compared to Stimulated 12 m D2 mice (Fig. 4e).

Restoration of Energy Homeostasis and Growth Factor Signaling

Energy homeostasis is important for proper neuronal signaling, and deficiencies in metabolism within the retina and optic nerve have been observed in the D2 model of glaucoma.[23] We measured the activation

(phosphorylation) of AMP-kinase (AMPK), a key metabolic regulator of ATP availability. We quantified the ratio of pAMPK to AMPK in the optic nerve (ON) and retina of Control and Stimulated 12 m D2, finding that the Stimulated group had significantly lower pAMPK/AMPK ratio than the Control 12 m D2 in both the ON and retina (Figs. 5a and 5b).

As BDNF is vital for RGC survival, we focused on BDNF and neurotrophin receptors TrkB and p75^{NTR}. Retinal BDNF increased with aging (Fig. 5c), but there was no difference between stimulation and control. Interestingly, the amount of TrkB receptor in retina was not different across the three groups (Control 3 m and Control and Stimulated 12 m D2; Fig. 5d). Phosphorylation of the TrkB receptor is an indication of its activity and binding of BDNF. Stimulated 12 m D2 retina had significantly greater TrkB phosphorylation than the Control 3 m D2 (Fig. 5e). Retinal p75^{NTR} in the Control 12 m D2 was significantly greater than that of the Control 3 m D2 and Stimulated 12 m D2 (Fig. 5f), indicating that TES reduced p75^{NTR} in Stimulated 12 m D2 to a level similar to that of the healthy Control 3 m D2 (Fig. 5f). Finally, we took the ratio of pTrkB to BDNF to understand how the receptor activation and BDNF levels related to each other across groups. We found that the pTrkB/BDNF ratio of the Stimulated 12 m

D2 retina was not different from the Control 3 m D2 retina (Fig. 5g), and both were higher than Control 12 m D2.

DISCUSSION

In this study, we probed the ability of TES to alter glaucoma pathological impacts on RGC and axon survival and to understand the mechanism of the changes observed. Interestingly, a protective effect of stimulation was observed in the RGC axons. Along with decreased axonal degeneration, TES treatment was able to restore energy homeostasis in the retina and optic nerve and decrease inflammation in the retina. Lastly, TES led to increased phosphorylation of TrkB and a decrease in p75[NTR].

Quiescent cells produce c-fos at undetectable levels; upon stimulation, transcription of c-fos is initiated.[43] The activation due to the TES was confirmed by the immunofluorescent detection of c-fos in the SC of D2 mice. The presence of c-fos in response to stimulation has long been used to map activity in the CNS, including the SC.[19] The c-fos activation found with TES was modest compared to the hypothalamic positive control, suggesting that further optimization of the stimulation paradigm may be warranted. It may be possible to achieve stronger c-fos activity in the superficial layers of the SC with an optimized paradigm and should be explored in the future.

After 8 weeks of TES, the Stimulated optic nerve had less degeneration than Control. Electrical stimulation has been previously shown to increase axonal regeneration.[45] For example, repetitive electrical stimulation promoted axonal outgrowth and regeneration after optic nerve crush. While these results were after trauma, they do demonstrate an axon-specific effect of electrical stimulation, which is similar to what was found here. Despite a greater number of axons in the Stimulated group, transport along RGC axons to the SC was significantly decreased in both the Stimulated and Control 12 m D2 compared to Control 5 m D2. The lack of increased axonal transport of CTB in the Stimulated group in spite of higher axon numbers suggests that axons may have been present and yet nonfunctional. This possibility fits within the timeframe of pathology in the D2 mouse model of glaucoma that shows loss of anterograde transport by 9 months of age.[13] In our study, mice were analyzed at 12 months of age, a time well beyond measurable anterograde axon transport deficit that corresponds to significant RGC and axon loss.[31]

The energy-demanding RGCs are particularly vulnerable to ATP decrease, which has been previously observed in 6 month-old D2 mice,[5] prior to axon structural pathology,[25] and axon transport deficit.[13] Energy decrease leads to activation of AMPK, a master cellular energy sensor and metabolism regulator.[18] Here, a significant increase in the ratio of activated pAMPK to inactive AMPK was detected in Control 12 m D2 optic nerve and retina, indicating a lack of ATP. TES rescued ATP decrease, as reflected by the significant reduction in the ratio of pAMPK to AMPK in Stimulated 12 m D2 optic nerve and retina. Modulation of metabolic pathways has been previously shown to be protective of RGCs, via expanding the energy substrate availability to RGCs in glaucoma,[23] or promoting insulin signaling after axotomy.[1] Interestingly, insulin growth factor-1 (IGF-1) upregulation contributed to RGC survival after optic nerve crush and TES.[33] Both insulin and IGF-1 led to the upregulation of mTOR, promoting protein synthesis and growth. While we did not evaluate IGF-1, future studies should investigate its importance given our finding that TES could promote energy homeostasis. Further investigation would be needed to determine the exact relationship between stimulation and improvement of ATP availability.

Neuroinflammation contributes to glaucoma through the activation and proliferation of microglia,[24] and T cell infiltration.[8] Microglia are the resident immune cells of the central nervous system, capable of responding to threats and maintaining homeostasis. Microglial activation is one of the earliest events and a critical contributor to glaucoma progression[6]; quantitative correlations between microglial activation and axon loss have also been documented in D2 mice.[46] Given the extent of inflammatory contribution to D2 pathology, we evaluated microglia and T cells in Control and Stimulated retina. TES reduced both Iba^{+} and CD3^{+} cells. Similar findings showed reduction in number and size of Iba1^{+} microglia in the cerebral cortex of rats following electrical stimulation,[3] mirroring the reduction of inflammatory cells found in our study. However, the mechanism behind such inhibition remains unknown. One study suggested attenuation of microglial invasion via glial cell-derived neurotrophic factor in ischemic brains of rats,[28] highlighting a possible relationship between inflammatory cells and neurotrophic factors. Future work is needed to understand if growth factors are related to the reduction of inflammatory response.

It is well established that BDNF-TrkB signaling promotes neuronal survival by activation of pro-survival pathways, and treatments that agonize the TrkB receptor are protective in glaucoma.[4,34] The BDNF-TrkB pathway has been found to have spatial and temporal changes for proper development,[14,44] with acute optic nerve injury,[17,38] and with chronic diseases such as glaucoma.[21] However, the direct application of
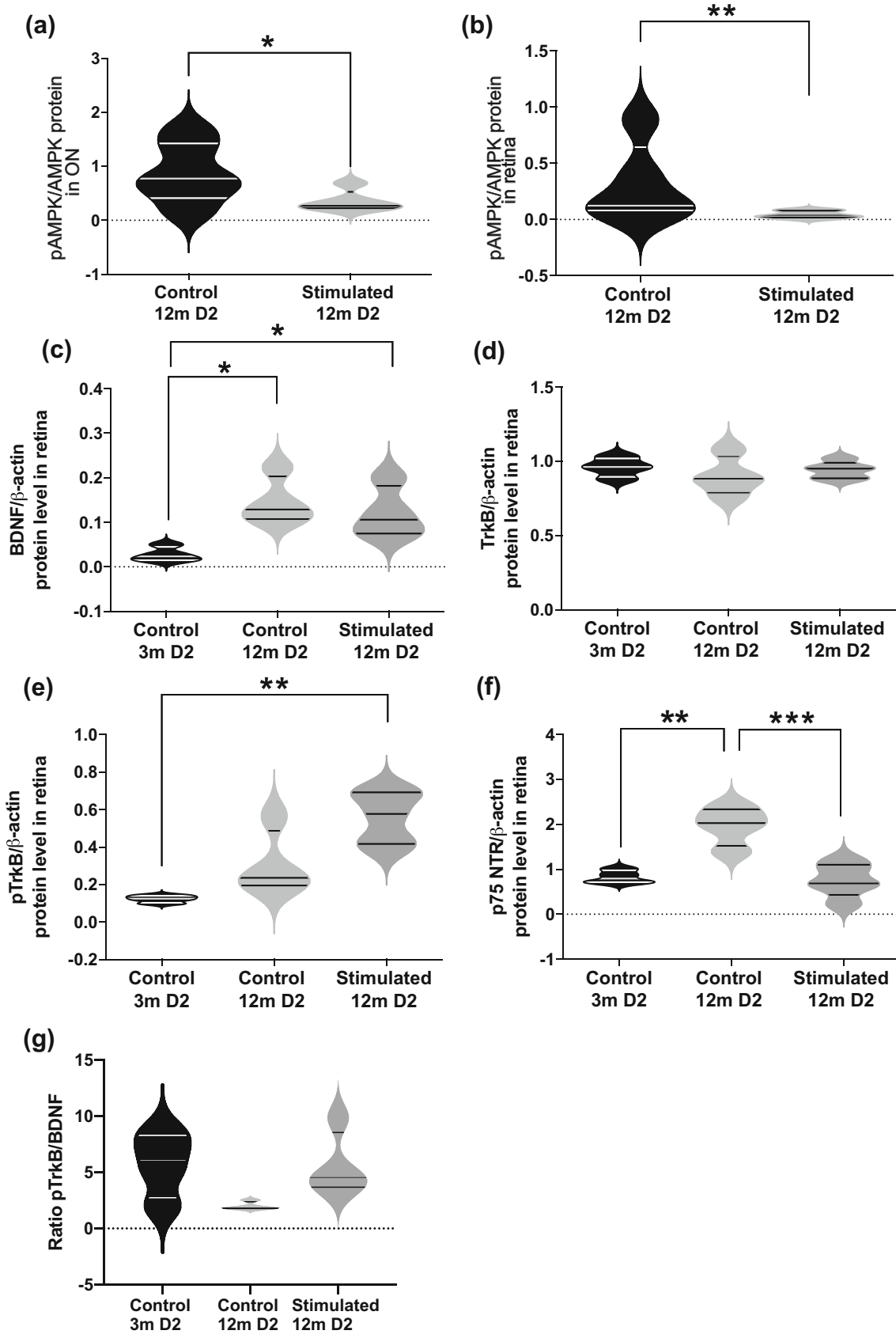
◄FIGURE 5. TES improves energy availability and increases TrkB phosphorylation. (a) A significant decrease of the pAMPK/AMPK protein ratio was found in the Stimulated 12 m D2 ON ($n = 6$) compared to Control 12 m D2 ON ($n = 5$), $p = 0.0432$. (b) Stimulated 12 m D2 retina ($n = 6$) has significantly lower pAMPK/AMPK ratio compared to Control 12 m D2 retina ($n = 5$), $p = 0.0087$. (c) BDNF is significantly increased in Control 12 m D2 ($n = 4$) and Stimulated 12 m D2 ($n = 4$) retina compared to Control 3 m D2 ($n = 4$) retina ($p = 0.0138$ and $p = 0.0462$). (d) No significant changes were detected in TrkB protein in Stimulated 12 m D2 retina ($n = 5$) compared to Control 12 m D2 ($n = 4$) and 3 m D2 retina ($n = 4$). (e) pTrkB protein was increased in the Stimulated 12 m D2 ($n = 5$) retina compared to Control 3 m D2 ($n = 4$) and 12 m D2 compared to Control 3 m D2 ($n = 4$) and 12 m D2 ($n = 4$) retina ($p = 0.0058$). (f) The amount of p75NTR protein was significantly increased in Control 12 m D2 ($n = 4$) retina compared to Control 3 m D2 ($n = 4$) ($p = 0.0023$), but TES led to a significant decrease of p75NTR protein in the Stimulated 12 m D2 ($n = 5$) compared to Control 12 m D2 retina ($n = 6$; $p = 0.0010$). (g) The ratio of pTrkB to BDNF shows no difference across the three groups.

neurotrophins has its own challenges as treatment options,[12,30] and options to stimulate endogenous production may better facilitate long-term treatment. While electrical stimulation has been found to upregulate BDNF in some neurons after axotomy,[2] the effect on TrkB is less clear. As with other neurotrophins, BDNF has multiple cellular receptors, including neurotrophin receptor p75[NTR]. p75[NTR] is dysregulated in glaucoma models[9] and has been shown to induce neuronal apoptosis.[22] Therefore, we characterized changes to BDNF and its two potential receptors, TrkB and p75[NTR], after TES. The amount of BDNF was significantly increased with age, but unchanged with TES. While the total amount of TrkB was unchanged with age or stimulation, activated pTrkB was significantly higher only in Stimulated 12 m D2 retina compared to the young Control. Interestingly, the amount of p75NTR was significantly decreased in the TES group compared to age matched control, and was not significantly different than the young control. Ultimately, the ratio of pTrkB to BDNF was the same in the young controls as TES stimulated animals. Taken together, these results indicated a potential pathway for support in the retina caused by TES. With these results, we hypothesize that p75[NTR] binding to BDNF in the Control group reduced the available BDNF for binding to TrkB, in turn reducing the phosphorylated TrkB and promoting cell death. In the Stimulated 12 m D2 retina where p75[NTR] levels were significantly reduced, more BDNF was available to activate and phosphorylate TrkB and induce survival signaling.

In conclusion, our results indicated that TES enhanced energy homeostasis, reduced inflammation, and decreased p75[NTR] availability in retina of the aged animals. TES also impacted the ON, with enhanced energy homeostasis and decreased degeneration. These changes are proven elements for RGC and ON survival, suggesting that TES is a viable approach for limiting glaucomatous damage. Deepening our understanding of the underling mechanism by which TES is rescuing RGCs and modulating inflammation and metabolism will provide the framework to justify application of TES in the clinic. Optimization of the stimulation paradigm may lead to greater improvement in RGC and ON support for reduced pathology and improved function.

AUTHOR CONTRIBUTIONS

Jassim, Cavanaugh, and Stukel, performed the experiments; Jassim and Cavanaugh undertook data analysis and writing. Willits and Inman conceived the experiments, supported data analysis, interpretation, and writing.

REFERENCES

[1]Agostinone, J., L. Alarcon-Martinez, C. Gamlin, W. Q. Yu, R. O. L. Wong, and A. Di Polo. Insulin signalling promotes dendrite and synapse regeneration and restores circuit function after axonal injury. *Brain* 141:1963–1980, 2018.

[2]Al-Majed, A. A., T. M. Brushart, and T. Gordon. Electrical stimulation accelerates and increases expression of BDNF and trkB mRNA in regenerating rat femoral motoneurons. *Eur. J. Neurosci.* 12:4381–4390, 2000.

[3]Baba, T., M. Kameda, T. Yasuhara, T. Morimoto, A. Kondo, T. Shingo, N. Tajiri, F. Wang, Y. Miyoshi, C. V. Borlongan, M. Matsumae, and I. Date. Electrical stimulation of the cerebral cortex exerts antiapoptotic, angiogenic, and anti-inflammatory effects in ischemic stroke rats through phosphoinositide 3-kinase/Akt signaling pathway. *Stroke* 40:e598–605, 2009.

[4]Bai, Y., J. Xu, F. Brahimi, Y. Zhuo, M. V. Sarunic, and H. U. Saragovi. An agonist TrkB mAb causes sustained TrkB activation, delays RGC death, and protects the

retinal structure in optic nerve axotomy and in glaucoma. *Invest. Ophthalmol. Vis. Sci.* 51:4722–4731, 2010.

[5]Baltan, S., D. M. Inman, C. A. Danilov, R. S. Morrison, D. J. Calkins, and P. J. Horner. Metabolic vulnerability disposes retinal ganglion cell axons to dysfunction in a model of glaucomatous degeneration. *J. Neurosci.* 30:5644–5652, 2010.

[6]Bosco, A., M. R. Steele, and M. L. Vetter. Early microglia activation in a mouse model of chronic glaucoma. *.J Comp. Neurol.* 519:599–620, 2011.

[7]Buckingham, B. P., D. M. Inman, W. Lambert, E. Oglesby, D. J. Calkins, M. R. Steele, M. L. Vetter, N. Marsh-Armstrong, and P. J. Horner. Progressive ganglion cell degeneration precedes neuronal loss in a mouse model of glaucoma. *J. Neurosci.* 28:2735–2744, 2008.

[8]Chen, H., K. S. Cho, T. H. K. Vu, C. H. Shen, M. Kaur, G. Chen, R. Mathew, M. L. McHam, A. Fazelat, K. Lashkari, N. P. B. Au, J. K. Y. Tse, Y. Li, H. Yu, L. Yang, J. Stein-Streilein, C. H. E. Ma, C. J. Woolf, M. T. Whary, M. J. Jager, J. G. Fox, J. Chen, and D. F. Chen. Commensal microflora-induced T cell responses mediate progressive neurodegeneration in glaucoma. *Nat. Commun.* 9:3209, 2018.

[9]Coassin, M., A. Lambiase, V. Sposato, A. Micera, S. Bonini, and L. Aloe. Retinal p75 and bax overexpression is associated with retinal ganglion cells apoptosis in a rat model of glaucoma. *Graefes Arch. Clin. Exp. Ophthalmol.* 246:1743–1749, 2008.

[10]Cooper, M. L., S. D. Crish, D. M. Inman, P. J. Horner, and D. J. Calkins. Early astrocyte redistribution in the optic nerve precedes axonopathy in the DBA/2 J mouse model of glaucoma. *Exp. Eye Res.* 150:22–33, 2016.

[11]Coughlin, L., R. S. Morrison, P. J. Horner, and D. M. Inman. Mitochondrial morphology differences and mitophagy deficit in murine glaucomatous optic nerve. *Invest. Ophthalmol. Vis. Sci.* 56:1437–1446, 2015.

[12]Daly, C., R. Ward, A. L. Reynolds, O. Galvin, R. F. Collery, and B. N. Kennedy. Brain-Derived Neurotrophic Factor as a Treatment Option for Retinal Degeneration. *Adv. Exp. Med. Biol.* 1074:465–471, 2018.

[13]Dengler-Crish, C. M., M. A. Smith, D. M. Inman, G. N. Wilson, J. W. Young, and S. D. Crish. Anterograde transport blockade precedes deficits in retrograde transport in the visual projection of the DBA/2J mouse model of glaucoma. *Front. Neurosci.* 8:290, 2014.

[14]Frade, J. M., P. Bovolenta, J. R. Martínez-Morales, A. Arribas, J. A. Barbas, and A. Rodríguez-Tébar. Control of early cell death by BDNF in the chick retina. *Development* 124:3313–3320, 1997.

[15]Fujikado, T., T. Morimoto, K. Matsushita, H. Shimojo, Y. Okawa, and Y. Tano. Effect of transcorneal electrical stimulation in patients with nonarteritic ischemic optic neuropathy or traumatic optic neuropathy. *Jpn. J. Ophthalmol.* 50:266–273, 2006.

[16]Gall, C., S. Schmidt, M. P. Schittkowski, A. Antal, G. G. Ambrus, W. Paulus, M. Dannhauer, R. Michalik, A. Mante, M. Bola, A. Lux, S. Kropf, S. A. Brandt, and B. A. Sabel. Alternating current stimulation for vision restoration after optic nerve damage: a randomized clinical trial. *PLoS ONE* 11:e0156134, 2016.

[17]Gao, H., X. Qiao, F. Hefti, J. G. Hollyfield, and B. Knusel. Elevated mRNA expression of brain-derived neurotrophic factor in retinal ganglion cell layer after optic nerve injury. *Invest. Ophthalmol. Vis. Sci.* 38:1840–1847, 1997.

[18]Garcia, D., and R. J. Shaw. AMPK: mechanisms of cellular energy sensing and restoration of metabolic balance. *Mol. Cell* 66:789–800, 2017.

[19]Geeraerts, E., M. Claes, E. Dekeyster, M. Salinas-Navarro, L. De Groef, C. Van den Haute, I. Scheyltjens, V. Baekelandt, L. Arckens, and L. Moons. Optogenetic stimulation of the superior colliculus confers retinal neuroprotection in a mouse glaucoma model. *J. Neurosci.* 39:2313–2325, 2019.

[20]Gupta, N., T. Ly, Q. Zhang, P. L. Kaufman, R. N. Weinreb, and Y. H. Yucel. Chronic ocular hypertension induces dendrite pathology in the lateral geniculate nucleus of the brain. *Exp. Eye Res.* 84:176–184, 2007.

[21]Gupta, V., Y. You, J. Li, V. Gupta, M. Golzan, A. Klistorner, M. van den Buuse, and S. Graham. BDNF impairment is associated with age-related changes in the inner retina and exacerbates experimental glaucoma. *Biochim. Biophys. Acta* 1567–1578:2014, 1842.

[22]Harada, C., T. Harada, K. Nakamura, Y. Sakai, K. Tanaka, and L. F. Parada. Effect of p75NTR on the regulation of naturally occurring cell death and retinal ganglion cell number in the mouse eye. *Dev. Biol.* 290:57–65, 2006.

[23]Harun-Or-Rashid, M., N. Pappenhagen, P. G. Palmer, M. A. Smith, V. Gevorgyan, G. N. Wilson, S. D. Crish, and D. M. Inman. Structural and functional rescue of chronic metabolically stressed optic nerves through respiration. *J. Neurosci.* 38:5122–5139, 2018.

[24]Howell, G. R., I. Soto, X. Zhu, M. Ryan, D. G. Macalinao, G. L. Sousa, L. B. Caddle, K. H. MacNicoll, J. M. Barbay, V. Porciatti, M. G. Anderson, R. S. Smith, A. F. Clark, R. T. Libby, and S. W. John. Radiation treatment inhibits monocyte entry into the optic nerve head and prevents neuronal damage in a mouse model of glaucoma. *J. Clin. Invest.* 122:1246–1261, 2012.

[25]Inman, D. M., R. M. Sappington, P. J. Horner, and D. J. Calkins. Quantitative correlation of optic nerve pathology with ocular pressure and corneal thickness in the DBA/2 mouse model of glaucoma. *Invest. Ophthalmol. Vis. Sci.* 47:986–996, 2006.

[26]Jassim, A. H., and D. M. Inman. Evidence of hypoxic glial cells in a model of ocular hypertension. *Invest. Ophthalmol. Vis. Sci.* 60:1–15, 2019.

[27]John, S. W. M., R. S. Smith, O. V. Savinova, N. L. Hawes, B. Chang, D. Turnbull, M. Davisson, T. H. Roderick, and J. H. Heckenlively. Essential iris atrophy, pigment dispersion, and glaucoma in DBA/2J Mice. *IOVS* 39:1998, 1998.

[28]Kameda, M., T. Shingo, K. Takahashi, K. Muraoka, K. Kurozumi, T. Yasuhara, T. Maruo, T. Tsuboi, T. Uozumi, T. Matsui, Y. Miyoshi, H. Hamada, and I. Date. Adult neural stem and progenitor cells modified to secrete GDNF can protect, migrate and integrate after intracerebral transplantation in rats with transient forebrain ischemia. *Eur. J. Neurosci.* 26:1462–1478, 2007.

[29]Kaplan, S., S. Geuna, G. Ronchi, M. B. Ulkay, and C. S. von Bartheld. Calibration of the stereological estimation of the number of myelinated axons in the rat sciatic nerve: a multicenter study. *J. Neurosci. Methods* 187:90–99, 2010.

[30]Khatib, T. Z., and K. R. Martin. Neuroprotection in glaucoma: towards clinical trials and precision medicine. *Curr. Eye Res.* 45:327–338, 2020.

[31]Libby, R. T., M. G. Anderson, I. H. Pang, Z. H. Robinson, O. V. Savinova, I. M. Cosma, A. Snow, L. A. Wilson, R. S. Smith, A. F. Clark, and S. W. John. Inherited glaucoma in DBA/2J mice: pertinent disease features for studying the neurodegeneration. *Vis. Neurosci.* 22:637–648, 2005.

[32] Morimoto, T., T. Fujikado, J. S. Choi, H. Kanda, T. Miyoshi, Y. Fukuda, and Y. Tano. Transcorneal electrical stimulation promotes the survival of photoreceptors and preserves retinal function in royal college of surgeons rats. *Invest. Ophthalmol. Vis. Sci.* 48:4725–4732, 2007.

[33] Morimoto, T., T. Miyoshi, S. Matsuda, Y. Tano, T. Fujikado, and Y. Fukuda. Transcorneal electrical stimulation rescues axotomized retinal ganglion cells by activating endogenous retinal IGF-1 system. *Invest. Ophthalmol. Vis. Sci.* 46:2147–2155, 2005.

[34] Mysona, B. A., J. Zhao, and K. E. Bollinger. Role of BDNF/TrkB pathway in the visual system: therapeutic implications for glaucoma. *Expert Rev. Ophthalmol.* 12:69–81, 2017.

[35] Ni, Y. Q., D. K. Gan, H. D. Xu, G. Z. Xu, and C. D. Da. Neuroprotective effect of transcorneal electrical stimulation on light-induced photoreceptor degeneration. *Exp. Neurol.* 219:439–452, 2009.

[36] Oono, S., T. Kurimoto, R. Kashimoto, Y. Tagami, N. Okamoto, and O. Mimura. Transcorneal electrical stimulation improves visual function in eyes with branch retinal artery occlusion. *Clin. Ophthalmol.* 5:397–402, 2011.

[37] Park, H. Y., and C. K. Park. Alterations of the synapse of the inner retinal layers after chronic intraocular pressure elevation in glaucoma animal model. *Mol. Brian* 7:1–10, 2014.

[38] Peinado-Ramón, P., M. Salvador, M. P. Villegas-Pérez, and M. Vidal-Sanz. Effects of axotomy and intraocular administration of NT-4, NT-3, and brain-derived neurotrophic factor on the survival of adult rat retinal ganglion cells: a quantitative in vivo study. *Invest. Ophthalmol. Vis. Sci.* 37:489–500, 1996.

[39] Quigley, H. A., G. R. Dunkelberger, and W. R. Green. Chronic human glaucoma causing selectively greater loss of large optic nerve fibers. *Ophthalmology* 95:357–363, 1988.

[40] Sagdullaev, B. T., P. J. DeMarco, and M. A. McCall. Improved contact lens electrode for corneal ERG recordings in mice. *Doc. Ophthalmol.* 108:181–184, 2004.

[41] Sambhara, D., and A. A. Aref. Glaucoma management: relative value and place in therapy of available drug treatments. *Ther. Adv. Chronic Dis.* 5:30–43, 2014.

[42] Schneider, C., W. S. Rasband, and K. W. Eliceir. NIH image to ImageJ-5 years of image analysis. *Nat. Methods* 7:671–675, 2012.

[43] Sheng, M., and M. Greenberg. The regulation and function of C-Fos and other immediate early genes in the nervous system. *Neuron* 477–485:1990, 1990.

[44] Spalding, K. L., R. A. Rush, and A. R. Harvey. Target-derived and locally derived neurotrophins support retinal ganglion cell survival in the neonatal rat retina. *J. Neurobiol.* 60:319–327, 2004.

[45] Tagami, Y., T. Kurimoto, T. Miyoshi, T. Morimoto, H. Sawai, and O. Mimura. Axonal regeneration induced by repetitive electrical stimulation of crushed optic nerve in adult rats. *Jpn. J. Ophthalmol.* 53:257–266, 2009.

[46] Wei, X., K. S. Cho, E. F. Thee, M. J. Jager, and D. F. Chen. Neuroinflammation and microglia in glaucoma: time for a paradigm shift. *J. Neurosci. Res.* 97:70–76, 2019.

[47] Yin, H., H. Yin, W. Zhang, Q. Miao, Z. Qin, S. Guo, Q. Fu, J. Ma, F. Wu, J. Yin, Y. Yang, and X. Fang. Transcorneal electrical stimulation promotes survival of retinal ganglion cells after optic nerve transection in rats accompanied by reduced microglial activation and TNF-alpha expression. *Brain Res.* 1650:10–20, 2016.